The Rangeland Hydrology and Erosion Model: A Dynamic Approach for Predicting Soil Loss on Rangelands

Mariano Hernandez[1], Mark A. Nearing[1], Osama Z. Al-Hamdan[2], Frederick B. Pierson[3], Gerardo Armendariz[1], Mark A. Weltz[4], Kenneth E. Spaeth[5], C. Jason Williams[1], and Carl L. Unkrich[1]

[1]USDA, Agricultural Research Service, Southwest Watershed Research Center, Tucson, Arizona, USA

[2]Texas A&M University-Kingsville, Kingsville, Texas, USA

[3]USDA, Agricultural Research Service, Northwest Watershed Research Center, Boise, Idaho, USA

[4]USDA, Agricultural Research Service, Exotic and Invasive Weeds Research Unit, Reno, Nevada, USA

[5]USDA, Natural Resources Conservation Service, Central National Technology Support Center, Ft. Worth, Texas, USA

Corresponding author: Mariano Hernandez (Mariano.Hernandez@ars.usda.gov)

Key Points:

- List up to three key points (at least one is required)
- Key Points summarize the main points and conclusions of the article
- Each must be 140 characters or less with no special characters or acronyms.

The Rangeland Hydrology and Erosion Model (RHEM) is a process-based erosion prediction tool specific for rangeland application, based on fundamentals of infiltration, hydrology, hydraulics, and erosion mechanics. RHEM captures the influence of plant lifeform type, vegetation foliar and ground cover, rock cover, slope steepness, soil texture, and rainfall on the dominant erosion processes on rangelands. The model utilizes a partial differential equation that solves in downslope distance and time during the event. Here we present the new dynamic model and evaluate it against 23 observed runoff and sediment events collected in a shrub-dominated semiarid watershed in the Arizona, USA. To evaluate the model, primary model parameters were determined using RHEM parameter estimation equations. Second, the model was calibrated to measurements from the watershed. The parameters estimated by the parameter estimation equations were within the lowest and highest values of the calibrated parameter set. Third, 124 data points in Arizona and New Mexico were used to evaluate runoff and erosion as a function of foliar canopy cover and ground cover. The dependence of average sediment yield on surface ground cover was moderately stronger than that on foliar canopy cover. The RHEM model is shown to track runoff volume, peak runoff, and sediment yield with sufficient accuracy for operational use of the model.

1 Introduction

The complex interactions of climate change processes, vegetation characteristics, surface soil processes, and human activities have major impacts on runoff and soil erosion processes on rangeland ecosystems. These processes and activities affect ecosystem function over a wide range of spatial and temporal scales [Williams *et al*., 2016]. Nearing *et al*. [2004] suggested that climatic variability will increase in the future. That is, global warming is expected to lead to a more vigorous hydrological cycle, including total rainfall and more frequent high-intensity rainfall events [Nearing *et al*., 2004]. Rangeland degradation is more likely to occur during these extreme rainfall events. Decades of research have shown that rangelands can sustainably produce a variety of goods and services even in the face of extreme climatic events if managers respond quickly and appropriately to changes [Havstad *et al*., 2009]. While individual ranchers may not be able to reduce the progress of climate change through mitigation, they may be able to adjust to climate change and devise management practices that are more resilient to climate impacts. Soil erosion is among the climate-related impacts that concern rangeland managers since conservation of topsoil is critical to sustained productivity in rangeland ecosystems. Soil loss rates on rangelands are regarded as one of the few quantitative indicators for assessing rangeland health and conservation practice effectiveness [Nearing *et al*., 2011].

According to Briske *et al*. [2011], the environmental benefits of grazing lands conservation practices have not previously been quantified at a national scale. The Rangeland Conservation Effects Assessment Project (CEAP) was formally initiated in 2006 to evaluate conservation effectiveness on rangelands and grazed forest that together comprise 188 million hectares of USA nonfederal rural land, as well as large areas of federal land in the western United States. Broad-scale assessments of this type rely on reliable modeling capabilities. According to Nearing and Hairsine [2011], future erosion prediction technology must be capable of simulating the complex interactions between vegetation characteristics, surface soil properties and hydrologic and erosion processes on rangelands. Furthermore, Al-Hamdan *et al*. [2012b] pointed out that better representation of the temporal dynamics of soil erodibility related to disturbed rangeland conditions (e.g., fire) is also needed.

In 2006, the USDA-Agricultural Research Service (USDA-ARS) developed the Rangeland Hydrology and Erosion Model (RHEM) V1.0 based on state-of-the-art technology from the Water Erosion Prediction Project (WEPP) [Flanagan and Nearing, 1995]. However, the basic equations in the WEPP model are based on experimental data from croplands. While many of the fundamental hydrologic and erosion processes can be expressed in a common way on both crop and rangelands, there were several aspects of the WEPP model that are not optimum for rangeland application and were modified, dropped, or replaced in RHEM [Nearing *et al*., 2011].

RHEM V1.0 was initially developed for undisturbed rangelands where the impact of concentrated flow erosion is limited and most soil loss occurs by rain splash and sheet erosion processes. RHEM V1.0 included a new splash and sheet equation developed by Wei *et al*. [2009] based on rainfall simulation data collected on rangeland plots from the WEPP and IRWET [IRWET and NRST, 1998] projects, which together covered 49 rangeland sites distributed across 15 western states. Also, it was incorporated the full solution to the kinematic wave equation for overland flow routing instead of the approximate method for calculating peak runoff implemented in WEPP [Stone *et al*., 1992]. Furthermore, RHEM V1.0 adapted the WEPP's steady state cropland-based shear stress approach for modeling concentrated flow erosion. Consequently, it was not possible to quantify within-storm sediment dynamics [Bulygina *et al*., 2007]. That is, a steady state model does not provide information on peak sediment discharge or the sediment load pattern within the storm, both of which can be useful for assessing potential pollution loadings from sediment fluxes into water courses and identifying sediment sources for designing appropriate management alternatives that reduce sediment losses [Kalin *et al*., 2004]. RHEM V1.0 uses the shear stress partitioning detachment and deposition concepts developed by Foster [1982], which distributes the transport capacity among various particle types.

The enhanced RHEM V2.3 model discussed herein provides major advantages over existing erosion model prediction technology, including RHEM V1.0. RHEM V2.3 is capable of capturing the influence of different plant types, disturbances such as fire, climate change, and rangeland management practices on important erosion processes acting on rangelands. RHEM has undergone continued review and expansion of capabilities. The most significant between this model and the original are: (1) The model uses a dynamic solution of the sediment continuity equation based on kinematic wave routing of runoff, and the integration of the newly developed splash and sheet source term equation and stream power for predicting sediment transport of concentrated flow erosion. (2) It integrates the approach for estimating the splash and sheet erodibility coefficient formulated by Al-Hamdan *et al*. [2016], who developed equations to predict the differences of erodibility before and after disturbance across a wide range of soil texture classes and vegetation cover types. (3) The model integrates the method for predicting concentrated flow erosion based on the work by Al-Hamdan *et al*. [2013], who developed a dynamic erodibility approach for modeling concentrated flow erosion (e.g., for sites with relatively immediate disturbance, such as fire). (4) The model includes a user-friendly web-based interface to allow users to simplify the use of RHEM, manage scenarios, centralize scenario results, compare scenario results, and provide tabular and graphical results [Hernandez *et al.*, 2015].

RHEM has been applied successfully to illustrate the influence of plant and soil characteristics on soil erosion and hydrologic function in MLRA 41 located in Southeastern Basin and Range region of the southern U.S. [Hernandez *et al.*, 2013]; assess non-federal western rangeland soil loss rates at the national scale for determining areas of vulnerability for accelerated soil loss using USDA Natural Resources Conservation Services(NRCS) National Resources Inventory(NRI) data [Weltz *et al.*, 2014]; predict runoff and erosion rates for refinement and development of Ecological Site Descriptions [Williams *et al.*, 2016]; characterize rangeland conditions based on a probabilistic approach subject to the presence of a set of soil erosion thresholds [Hernandez *et al*. 2016].

The objectives of this study were as follows. (1) to present the driving equations for the new RHEM V2.3 model; (2) to calibrate the new RHEM V2.3 model using 23 rainfall-runoff-sediment yield events on a small semiarid sub-watershed within the Walnut Gulch Experimental Watershed in Arizona, and compare them against parameters estimated by the RHEM parameter estimation equations; (3) to examine the ranges of parameter values from RHEM parameter estimation equations and compare them to calibrated parameter values; (4) to evaluate the overall influence of foliar canopy cover, ground surface cover, and annual rainfall on soil erosion rates from rangelands using 124 NRI plots in Arizona and New Mexico.

2. Material and Methods

This section is divided into four main parts as follows. (1) Presentation of fundamental hydrologic and erosion equations in RHEM, (2) An overview of the RHEM parameter estimation equations, (3) Model calibration with the Model-Independent **P**arameter **EST**imation (PEST) program, (4) Statistical analysis.

2.1. Fundamental hydrologic and erosion equations

2.1.1. Overland flow model

The hydrology component of the enhanced RHEM model is based on the KINEROS2 model [Smith *et al.*, 1995]. The model was implemented to simulate one-dimensional overland flow within an equivalent plane representing an arbitrarily shaped hillslope with uniform or curvilinear slope profiles. The flow per unit width across a plane surface as a result of rainfall can be described by the one-dimensional continuity equation [Woolhiser *et al*. 1990].

$$\frac{\partial h}{\partial t} + \frac{\partial q}{\partial x} = \sigma(x, t) \qquad (1)$$

where h is the flow depth at time t and the position x; x is the space coordinate along the direction of flow; q is the volumetric water flux per unit plane width ($m^2\ s^{-1}$); and σ (x, t) is the rainfall excess ($m\ s^{-1}$).

$$\sigma(x,t) = r - f \qquad (2)$$

where r is the rainfall rate (m s^{-1}), and f is the infiltration rate (m s^{-1}). The following equation represents the relationship between q and h:

$$q = \left(\frac{8gS}{f_t}\right)^{1/2} h^{3/2} \qquad (3)$$

where g is the gravity acceleration (m s^{-2}), S is the slope (m m^{-1}), and f_t is the total friction factor estimated by [Al-Hamdan *et al.*, 2013]. Substituting Equations (2) and (3) in Equation (1) results in the hydrology routing equation:

$$\frac{\partial h}{\partial t} + \frac{3}{2}\left(\frac{8gS}{f_t}\right)^{1/2} h^{1/2} \frac{\partial h}{\partial x} = r - f \qquad (4)$$

In RHEM, for a single plane, the upstream boundary is assumed to be at zero depth and the downstream boundary is a continuing plane (along the direction of flow).

$$h(0,t) = 0 \qquad (5)$$

The infiltration rate is computed in KINEROS2 using the three-parameter infiltration equation [Parlange *et al.*, 1982], in which the models of Green and Ampt [1911] and Smith and Parlange [1978] are included as two limiting cases.

$$f = K_e \left[1 + \frac{\alpha}{exp\left(\frac{\propto I}{G\Delta\theta_i}\right) - 1}\right] \qquad (6)$$

where I is the cumulative depth of the water infiltrated into the soil (m), K_e is the surface effective saturated hydraulic conductivity (m s^{-1}), G (m) accounts for the effect of capillary forces on moisture absorption during infiltration, and α is a scaling parameter. When α=0, Equation 6 is reduced to the simple Green and Ampt infiltration model, and when α=1, the equation simplifies to the Parlange model. Most soil exhibit infiltrability behavior intermediate to these two models, and KINEROS2 uses a weighting α value of 0.85 [Smith *et al.*, 1993]. The state variable for infiltrability is the initial water content, in the form of the soil saturation deficit, $B = G(\theta_s - \theta_i)$, defined as the saturated moisture content minus the initial moisture content. The saturation deficit $(\theta_s - \theta_i)$ is one parameter because θ_s is fixed from storm to storm. For ease of estimation, the KINEROS2 input parameter for soil water is a scaled moisture content, S=θ/ϕ, (ϕ is the soil porosity) which varies from 0 to 1. Thus initial soil conditions are represented by the variable S_i (=θ_i/ϕ). Thus, there are two parameters, K_e, and G to characterize the soil, and the variable S_i to characterize the initial condition

2.1.2. Overland soil erosion, deposition, and transport

The RHEM erosion model uses a dynamic sediment continuity equation to describe the movement of suspended sediment in a concentrated flow area [Bennett, 1974].

$$\frac{\partial(Ch)}{\partial t} + \frac{\partial(Cq_r)}{\partial x} = D_{ss} + D_{cf} \qquad (7)$$

Where C is the measured sediment concentration (kg m^{-3}), q_r is the flow discharge of concentrated flow per unit width (m^{-2} s^{-1}), D_{ss} is the splash and sheet detachment rate (kg s^{-1} m^{-1}), and D_{cf} is the concentrated flow detachment rate (kg s^{-1} m^{-2}). For a unit wide plane, when overland flow accumulates into a concentrated flow path, the following equation calculates the concentrated flow discharge per unit width (q_r):

$$q_r = \frac{q}{w} \qquad (8)$$

Where w is the concentrated flow width (m) calculated by [Al-Hamdan *et al.*, 2012a]

$$w = \frac{2.46\, Q^{0.39}}{S^{0.4}} \qquad (9)$$

The splash and sheet detachment rate (D_{ss}) is calculated by the following equation [Wei *et al.*, 2009]:

$$D_{ss} = K_{ss} r^{1.052} \sigma^{0.592} \qquad (10)$$

where K_{ss} is the splash and sheet erodibility, r (m s^{-1}) is the rainfall intensity and σ is rainfall excess (m s^{-1}).

Concentrated flow detachment rate (D_{cf}) is calculated as the net detachment and deposition rate [Foster, 1982]:

$$D_{cf} = \begin{bmatrix} D_c\left(1 - \frac{CQ}{T_c}\right), CQ \le T_c \\ \frac{0.5\, V_f}{Q}(T_c - CQ), CQ \ \ge T_c \end{bmatrix} \qquad (11)$$

where D_c is the concentrated flow detachment capacity (kg s^{-1} m^{-2}); Q is the flow discharge (m^3 s^{-1}); T_c is the sediment transport capacity (kg s^{-1}); and V_f is the soil particle fall velocity (m s^{-1}) that is calculated as a function of particle density and size [Fair *et al.*, 1971].

Sediment detachment rate from the concentrated flow is calculated by employing soil erodibility characteristics of the site and hydraulic parameters of the flow such as flow width and stream power. Soil detachment is assumed to start when concentrated flow starts (i.e. no threshold concept for initiating detachment is used) [Al-Hamdan *et al*., 2012b].

To calculate D_c, the equation developed by Al-Hamdan *et al*. [2012b] is used:

$$D_c = K_w(w) \qquad (12)$$

where K_w is the stream power erodibility factor ($s^2\ m^{-2}$) and w is the stream power ($kg\ s^{-3}$). We implemented the empirical equation developed by Nearing *et al*. [1997] to calculate the transport capacity (T_c).

$$Log_{10}\left(\frac{10T_c}{w}\right) = -34.47 + 38.61 * \frac{exp[0.845 + 0.412\log(1000w)]}{1 + exp[0.845 + 0.412\log(1000w)]} \qquad (13)$$

Soil detachment is assumed to be a nonselective process, so the sediment particles size distribution generated from actively eroding areas is assumed to be a function of the fraction of total sediment load represented by five particle classes based on soil texture. The transport capacity equation of Nearing *et al*. [1997] does not account for particle sorting. Consequently, routing of sediment by size particle is not carried out.

Several studies have documented increases in peak flows and erosion occurring on systems that have been altered by some disturbance. For example, at the plot/hillslope scale, factor increases in sediment delivery between 2- and 1000 -fold have been reported [Morris and Moses, 1987; Scott and Van Wyk, 1992; Shakesby *et al*., 1993; Cerda, 1998; Cannon *et al*., 2001; Pierson *et al*., 2002]. Results from rainfall simulator experiments suggest that erosion rates are much higher in the early part of a runoff event than in the latter part of the event on forest roads [Foltz *et al*., 2008] and burned rangeland [Pierson *et al*., 2008]. These rapid changes in the concentrated flow erosion rate on disturbed soils may be caused by the winnowing of fine or easily detached soil particles during the early stages of erosive runoff, thus leaving larger or more embedded particles and/or aggregates which require greater stream power for detachment [Robichaud *et al*., 2010].

RHEM also has the capacity, as an option, to use equations developed by Al-Hamdan *et al*. [2012b] for characterizing events with high concentrated flow erodibility at the onset of the event with exponentially decreasing erodibility because of the reduction of the availability of disturbance generated sediment.

$$D_c = K_{w(Max)adj}\,exp(\beta\ q_c)\omega \qquad (14)$$

$$q_c = \int q_r dt \qquad (15)$$

$$\omega = \gamma S q_r \qquad (16)$$

where $K_{\omega(Max)adj}$ is the maximum stream power erodibility ($s^2\ m^{-2}$) corresponding to the decay factor β = -5.53 (m^{-2}), β is a decay coefficient representing erodibility change during an event

(m^{-2}), ω is the stream power (kg s^{-3}), q_c is the cumulative flow discharge of concentrated flow per unit width (m^2), γ is the water specific weight (kg m^{-2} s^{-2}), and S is the slope (m m^{-1}).

2.2. RHEM Model Parameter Estimation Equations

An important aspect of RHEM about the application by rangeland managers is that it is parameterized based on plant growth form types using data that are typically collected for rangeland management processes (e.g. rangeland health or NRI assessments).

2.2.1. Effective saturated hydraulic conductivity

Research has indicated that infiltration, runoff, and erosion dynamics are correlated with the presence/absence and composition of specific plant taxa and growth attributes [Davenport *et al*., 1998, Wainwright *et al*., 2000, Ludwig *et al*., 2005, Peters *et al*., 2007, Turnbull *et al*., 2008, Turnbull *et al*., 2012, Petersen *et al*., 2009, Pierson *et al*., 2010, Pierson *et al*., 2013, Wilcox *et al*., 2012a and Williams *et al*., 2014]. It has been known that infiltration of rainfall on rangelands is increased with an increase of vegetal surface cover present. Tromble *et al*. [1974] evaluated infiltrability on three range sites in Arizona and found vegetal cover and litter biomass to be most positively related, whereas gravel cover was negatively related. Meeuwig [1970] and Dortignac and Love [1961] also found litter cover to be important. Work by Spaeth *et al*. [1996] concluded that plant species and ground cover effects significantly enhanced estimation of infiltration capacity compared to purely physically based predictions. The study by Thompson *et al*. [2010] provides a detail literature review about research that has been conducted concerning vegetation-infiltration relationships across climate and soil type gradients.

Soil texture may be used as the first estimator of K_e because texture affects the pore space available for water movement. Also, soil texture is easy to measure and often available for an area of interest. Rawls *et al*. [1982] developed a look-up table of K_s values for the 11 USDA soil textural classes. Bulk density is another basic soil property that is related to pore space and water movement. Rawls *et al*. [1998] revised the texture-based look-up table to include two porosity classes within each textural class, the geometric means of the K_s along with the 25% and 75% percentile values. The texture/porosity K_s estimates were based on a national database of measured K_s values and soil properties at 953 locations. These estimates indicate that (1) K_s is highest for coarse-textured soils and (2) within a textural class, soils with greater porosity (lower bulk density) have higher K_s values.

The geometric mean of K_s sorted according to the soil texture, and bulk density classes along with the 25% and 75% percentile values are presented in Table 3. Also, reported in Table 1 is the corresponding arithmetic mean porosity ϕ (m^3 m^{-3}) and mean capillary drive G (mm).

Table 1. Estimation guides for soil hydraulic properties based on sample data [Rawls *et al*., 1998]. The geometric mean of the Ks sorted according to soil texture and bulk density classes along with the 25% and 75% percentile.

USDA Soil Class Texture	Geometric Mean Ks (mm h^{-1})	75% (mm h^{-1})	25% (mm h^{-1})	Porosity (m^3 m^{-3})	Mean capillary drive G (mm)	Sand (%)	Clay (%)	Sample Size
Sand	181.9 91.4	266.8 218.5	96.5 64.0	0.44 0.39	50	92 91	4 4	39 30
Loamy Sand	123.0 41.4	195.5 77.6	83.8 30.5	0.45 0.37	70	82 82	6 7	19 28
Sandy Loam	55.8 12.8	129.6 31.3	30.5 5.1	0.47 0.37	130	65 68	11 13	75 112
Loam	3.9 6.2	28.4 16.5	1.6 2.8	0.47 0.39	110	38 43	23 22	44 65
Silt Loam	14.4 3.4	37.1 9.9	7.6 1.0	0.49 0.39	200	18 21	19 20	61 46
Sandy Clay Loam	7.7 2.8	50.5 10.9	2.0 1.0	0.44 0.37	260	56 58	26 26	20 53
Clay Loam	4.2 0.7	13.1 3.8	2.2 0.2	0.48 0.40	260	29 35	35 35	20 53
Silty Clay Loam	3.7 4.9	10.4 14.0	2.3 2.3	0.50 0.43	350	10 10	34 32	26 33
Sandy Clay	0.9	2.5	0.3	0.39	300	51	36	14
Silty Clay	1.8	7.5	0.5	0.53	380	4	49	10
Clay	2.0 1.8	6.0 6.9	0.9 0.3	0.48 0.40	410	18 26	53 50	20 21

Saturated hydraulic conductivity is known to be lognormally distributed in space [Nielsen *et al*., 1973; Smith and Goodrich, 2000; Nielsen and Wendroth, 2003], with variations of an order of magnitude or more across relatively short distances. It is clear that representing a landscape using various values of saturated conductivity distributed across space with a lognormal distribution is more realistic than a single uniformly applied mean value. The RHEM model defines a range of hydraulic conductivity values based on the 25% and 75% percentile values for each soil textural class reported in Table 1 [Rawls *et al*., 1998]. Then we adjusted them to account for the effects of litter and basal cover based on the exponential model developed by Stone *et al*. [1991]. Stone *et al*. [1991] developed an exponential model to adjust the baseline saturated hydraulic conductivity [Rawls *et al*., 1982] as a function of surface cover and canopy cover based on an unpublished analysis of rainfall simulator data on desert brush dominated sites in Arizona and Nevada. Moreover, they divided the baseline saturated hydraulic conductivity by two to account for the effects of crusting on the effective saturated hydraulic conductivity. However, Stone *et al*. [1991] did not report criteria to assess the goodness of fit of the model and the range of values of the predictor variables. In the model developed by Stone *et al*. [1991], the effective saturated hydraulic conductivity increases exponentially as ground cover and canopy cover increases, which is consistent with the trend shown in croplands reported by Rawls *et al*. [1990] and Zhang *et al*. [1995]. Moreover, as pointed out by Zhang *et al*. [1995], for accurate simulation of the effects of canopy cover on infiltration and runoff, the impact of canopy height must be considered.

RHEM estimates of effective saturated hydraulic conductivity are computed as follows:

$$K_{e_i} = K_{b_i}\, e^{[p_i(litter+basal)]} \qquad (17)$$

In this equation, K_{bi} is the 25% percentile saturated hydraulic conductivity for each soil textural class, *i*, listed in Table 1. *P* is defined as the natural log of the ratio of the 75% to the 25% percentile values of saturated hydraulic conductivity; *litter* is litter cover (%); and *basal* is basal area cover (%).

2.2.2. Hydraulic roughness coefficient

Al-Hamdan *et al*. [2013] developed empirical equations that predict the total measured friction factor (f_t) by regressing the total measured friction against the measured vegetation and rock cover, slope, and flow rate. The data used in their study were obtained from rangeland rainfall simulator experiments conducted by the USDA-ARS Northwest Watershed Research Center in Boise, Idaho. The data were collected from rangeland sites within the U.S. Great Basin region and a broad range of slope angles (5.6% to 65.8%), soil types, and vegetation cover. Many of these sites show some degree of disturbance and/or treatment, such as tree encroachment, prescribed fire, wildfire, tree mastication, and/or tree cutting. Average slope, canopy and ground cover, and micro-topography were measured for each plot [Pierson *et al*., 2007, 2009, 2010].

According to Al-Hamdan *et al*. [2013], total hydraulic friction was negatively correlated with flow discharge and the percentage of bare ground, and it was positively correlated with the presence of vegetation cover and slope. Equations that were developed from concentrated flow data have significantly different coefficients values compared to those obtained from sheet flow data. The flow discharge and slope in the total friction equation enhanced the prediction of the total friction, and consequently improved the estimation of the proportion of the assumed soil friction to total friction. All equations derived by Al-Hamdan *et al*. [2013] showed that basal plant cover was the most important effect on total friction among other cover attributes.

RHEM computes the total friction (f_t) factor estimated by [Al-Hamdan *et al*., 2013] as follows:

$$\log(f_t) = -0.109 + 1.425\, litter + 0.442\, rock + 1.764\,(basal + cryptogams) + 2.068\, S \qquad (18)$$

where *litter* is the fraction of area covered by litter to total area ($m^2\ m^{-2}$), *basal* + *cryptogams* is the fraction of area covered by basal plants and cryptogams to total area ($m^2\ m^{-2}$), and rock is the fraction of area covered by rock to total area ($m^2\ m^{-2}$), and *S* is the slope ($m\ m^{-1}$).

2.2.3. Splash and sheet erodibility factor

The RHEM model parameterization represents erosion processes on undisturbed rangelands, as well as rangelands that show disturbances such as fire or woody plant encroachment [Nearing *et al*., 2012; Hernandez *et al*. 2013; Al-Hamdan *et al*. 2016; Williams *et al*. 2016]. In RHEM, soil detachment is predicted as a combination of two erosion processes, rain splash and thin sheet flow (splash and sheet) detachment and concentrated flow detachment.

This section presents empirical equations developed by Al-Hamdan *et al*. [2016] using piecewise regression analysis to predict erodibility across a broad range of soil texture classes based on vegetation cover and surface slope steepness.

Bunch Grass:

$$\mathrm{Log}_{10}\, Kss = \left\{ \begin{array}{ll} 4.154 - 2.547 * G - 0.7822 * F + 2.5535 * S & \text{if } G \leq 0.475 \\ 3.1726975 - 0.4811 * G - 0.7822 * F + 2.5535 * S & \text{if } G > 0.475 \end{array} \right\} \quad (19)$$

Sod Grass:

$$\mathrm{Log}_{10}\, Kss = \left\{ \begin{array}{ll} 4.2169 - 2.547 * G - 0.7822 * F + 2.5535 * S & \text{if } G \leq 0.475 \\ 3.2355975 - 0.4811 * G - 0.7822 * F + 2.5535 * S & \text{if } G > 0.475 \end{array} \right\} \quad (20)$$

Shrub:

$$\mathrm{Log}_{10}\, Kss = \left\{ \begin{array}{ll} 4.2587 - 2.547 * G - 0.7822 * F + 2.5535 * S & \text{if } G \leq 0.475 \\ 3.2773975 - 0.4811 * G - 0.7822 * F + 2.5535 * S & \text{if } G > 0.475 \end{array} \right\} \quad (21)$$

Forbs:

$$\mathrm{Log}_{10}\, Kss = \left\{ \begin{array}{ll} 4.1106 - 2.547 * G - 0.7822 * F + 2.5535 * S & \text{if } G \leq 0.475 \\ 3.1292975 - 0.4811 * G - 0.7822 * F + 2.5535 * S & \text{if } G > 0.475 \end{array} \right\} \quad (22)$$

where G is the area fraction of ground cover, F is the area fraction of foliar cover, and S is the slope gradient (expressed as a fraction).

The performance of the model with the new parameterization schemes indicates that using K_{ss} alone, as the indicator of erodibility factor in RHEM, works reasonably well as long as concentrated flow paths work primarily as the transport tool of the splash and sheet-generated sediments. The default value for K_w was set as $7.7\text{x}10^{-6}$ ($s^2\ m^{-2}$) in the current RHEM V2.3. This small value of concentrated flow erodibility is typical for undisturbed rangeland. It is recommended to use the K_{ss} equation that represents the dominant vegetation community in the site to be evaluated. However, if the site does not have a dominant vegetation form or more details are needed, then weight averaging between equations (19) through (22) based on the percentage of life form would be used. Only in the special case of abrupt disturbance with steep slopes (> 20%) and high silt, would the parameterization of K_w (as described in Section 2.2.4) be needed.

2.2.4. Concentrated flow erodibility coefficients

The model employs two empirical functions developed by Al-Hamdan *et al*. (2012b) to calculate K_ω for a broad range of undisturbed rangeland sites and tree encroached sites.

$$log_{10}(K_w) = -4.14 - 1.28litter - 0.98rock - 15.16clay + 7.09silt \qquad (23)$$

$$log_{10}(K_w) = -4.05 - 0.81(litter + cryptogams + basal) - 11.87clay + 5.19silt \qquad (24)$$

The model also has the capacity, as an option, to use equations developed by Al-Hamdan *et al*. [2012b] for predicting maximum erodibility for a wide range of burned rangeland sites including burned tree encroached sites.

$$log_{10}\left(K_{w(\max)adj}\right) = -3.28 - 1.77litter - 1.26rock - 2.46(basal + crypto) + 3.53silt \qquad (25)$$

$$log_{10}\left(K_{w(\max)adj}\right) = -3.64 - 1.97(litter + basal + crypto) - 1.85rock - 4.99clay + 6.0silt \qquad (26)$$

where *litter, basal, and crypto* are the fraction of area covered by litter, basal, and cryptogam to total area (m^2 m^{-2}), *rock* is the fraction of area covered by rock to the total area (m^2 m^{-2}), and *clay* and *silt* fraction.

2.3. PEST model parameterization

This study employs PEST software [Doherty, 2005] to calibrate RHEM parameters and evaluate model performance for the 23 rainfall-runoff-erosion events at LH106. The parameter calibration process included two approaches: first, the overland flow related parameters were calibrated (effective saturated hydraulic conductivity, total friction factor, capillary drive, and saturation). The parameters slope, coefficient of variation for K_e, and Interception were held constant during the calibration. A detailed description of the overland flow parameters can be found in Smith *et al*. [1995]; second, the calibration of the splash-and-sheet soil erodibility coefficient was achieved by keeping constant the optimized overland flow parameters.

2.4. Statistical analysis

Nash-Sutcliffe Efficiency (NSE) [Nash and Sutcliffe, 1970] between observed and calculated cumulative flows was calculated for each single event at LH106 as follows:

$$NSE = 1 - \frac{\sum_{t=1}^{T}(O_t - M_t)^2}{\sum_{t=1}^{T}(O_t - \bar{O})^2} \qquad (27)$$

where O_t, $\bar{O}$ and M_t are observed cumulative flows at time step t, average cumulative value, and modeled cumulative flows at time step t, respectively. T is the total number of time steps in the simulation for each rainfall event.

Moreover, percent bias (PBIAS) [Gupta *et al*., 1999] and the RMSE-observations standard deviation ratio (RSR) [Moriasi *et. al*., 2007] were calculated to evaluate the overall performance of the model for runoff volume, peak runoff, and sediment yield estimates from the 23 events at LH106.

PBIAS was calculated by

$$PBIAS = \frac{\sum_{i=1}^{N}(O_i - M_i) * 100}{\sum_{i=1}^{N} O_i} \qquad (28)$$

RSR was calculated by

$$RSR = \frac{\sqrt{\sum_{i=1}^{N}(O_i - M_i)^2}}{\sqrt{\sum_{i=1}^{N}(O_i - \bar{O})^2}} \qquad (29)$$

where O_i is the observed value of event i; M_i is the model generated value for the corresponding event i; $\bar{O}$ is the average of the observed values, and N is the total number of events at LH106.

3. Study Area and NRI database

3.1. Lucky Hills 106 watershed

The data used for the calibration and evaluation of the model were obtained from the USDA-ARS Southwest Watershed Research Center's Lucky Hills experimental site, located in the Walnut Gulch Experimental Watershed (WGEW). The semiarid WGEW is located in southeastern Arizona (31^{o} 43'N, 110^{o} 41'W) and surrounds the town of Tombstone, Arizona (Fig. 1). It has a mean annual temperature of 17.7^{o}C and a mean annual precipitation of 350 mm, the majority of which is a result of high-intensity convective thunderstorms in the summer monsoon season [Keefer *et al*., 2015].

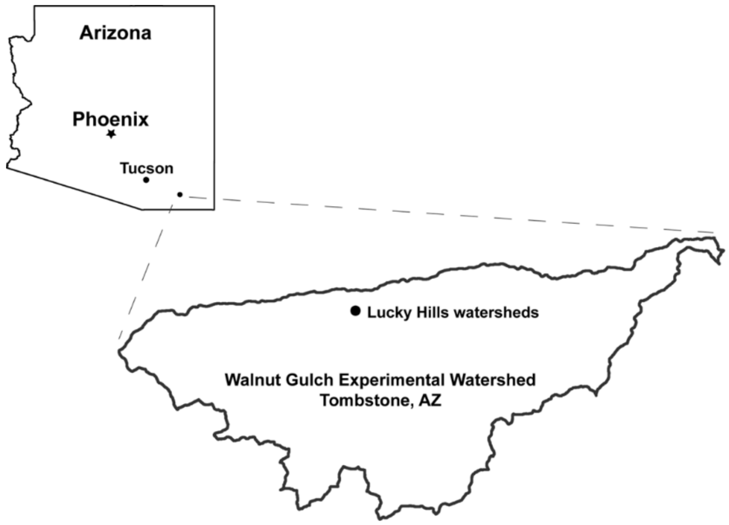

Figure 1. Location of the Lucky Hills subwatershed study area within the Walnut Gulch Experimental Watershed.

The Lucky Hills 106 (LH106) subwatershed has an area of 0.367 hectares. The LH106 subwatershed presents an excellent location for this study because of the availability of rainfall, runoff, Time Domain Reflectometry (TDR) sensors placed at each rain gauge for estimating gravimetric soil moisture, and sediment time-series data required for model calibration at the hillslope scale. It also is appropriate because it is not highly channelized and acts more as a large hillslope rather than a watershed with significant contribution of channel sediment [Nichols *et al*., 2012]. At this scale, rainfall amount and intensity, vegetative canopy cover, ground surface cover, and micro-topography (and their spatial variability) largely determine overland flow and soil erosion processes [Lane *et al*., 1997]. Rainfall is recorded at Rain Gauge 83 with a temporal resolution of 1 min (Fig. 2). A 1m x 1m DEM was prepared based on LIDAR survey and used to relate to micro-topography characteristics.

The vegetation is comprised mostly of shrubs on an 8% slope. Dominant shrubs include Creosote [Larrea tridentata (Sessé & Moc. ex DC.) Coville] and Whitethorn [Acacia constricta Benth.]. Foliar and ground cover information is given in Table 2. The soil is a Lucky Hills-McNeal sandy loam complex with approximately 52% sand, 26% silt, and 22% clay on a Limy Uplands (12-16"p.z.) ecological site. Rainfall and runoff data have been collected at Lucky Hills since 1963 when rain gauge 83 and weirs LH 104 and 102 were installed (Fig. 2). Rain gauge 84 was added in 1964, when an H-flume was installed on LH106 in 1965 (Fig. 2), with integrated depth pump samplers added in 1973 to collect suspended sediment samples in addition to the coarse load deposited in the flume during each event [Simanton *et al*., 1993]. Since the instrumentation was installed in the early 1960's, rainfall and runoff data have been collected with only short interruptions for upgrading equipment, which occurred during the winter [Renard *et al*., 1980]. Sediment data are prone to periodic sampling errors, so sediment data are not available for many events for which rainfall and runoff data are available [Nearing *et al*., 2007].

Table 2. Summary of the ground surface and foliar canopy cover for Lucky Hills 106 subwatershed.

Cover			
Ground Surface	**(%)**	**Foliar Canopy**	**(%)**
Basal	3	Bunch Grass	1
Rock	45	Forbs/Annual Grasses	2
Litter	10	Shrub	35
Cryptogams	0	Sod Grass	0
Total	**58**	**Total**	**38**

We used 23 time-intensity pairs collected between 2005 and 2010 from Rain Gauge 83 as an input into the RHEM model to assess the hydrologic and erosion response of LH106 (Fig. 2). Summary descriptive statistics of rainfall, observed runoff volume, observed peak runoff, and observed sediment yield are presented in Table 3.

Table 3. Summary descriptive statistics of the 23 events at Lucky Hills 106 and Rain Gauge 83.

	Mean	Min	Max	Std
Rainfall Volume (mm)	21.86	8.64	46.35	12.08
Runoff Volume (mm)	7.63	2.10	22.82	6.06
Peak Runoff Rate (mm h^{-1})	38.34	11.92	106.56	24.01
Sediment Yield (t ha^{-1})	0.23	0.03	0.94	0.23

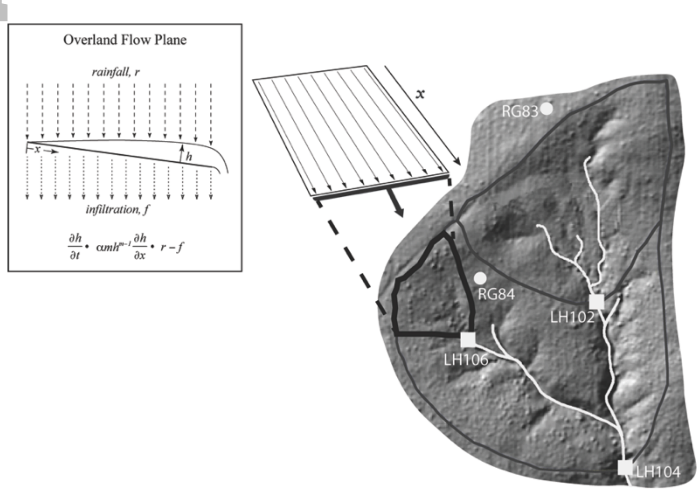

Figure 2. Lucky Hills 106 and its representation as overland flow plane in the RHEM model.

3.2. National Resources Inventory Field Measurements and Data Description

A major data source for rangeland assessment on non-federal lands is the National Resource Inventory (NRI) [Goebel and Schmude, 1980]. The USDA-NRCS provided data for 542 NRI points collected between 2003 and 2014 across Arizona, New Mexico, and Utah to parameterize the RHEM model. The points were grouped by soil texture classes, as follows: sand, sandy loam, silt loam, and clay loam. For this study, we selected only the sandy loam soil texture class to be in agreement with the LH106 soil texture class. We found 124 NRI points in the sandy loam group. Furthermore, the 124 NRI data points were further grouped into annual rainfall regimes measured at five weather stations. The Jornada weather station is located in New Mexico, and Ganado, Laveen, Snowflake, and Willcox are in Arizona.

Next, ground surface cover, foliar cover, basal area, cryptogams cover, litter cover, rock fragment cover, and slope gradient percent were estimated from the 124 NRI points. Figures 3, 4, and 5 present the distributions for ground surface cover, foliar canopy cover, and slope steepness grouped by annual rainfall amounts. For purposes of RHEM application, ground cover is the cover of the soil surface that essentially is in contact with the soil, as opposed to canopy cover or foliar cover, which is cover above the ground surface. Ground cover may be present in the form of plant litter, rock fragments, cryptogams, and basal plant areas. A comprehensive review of the NRI inventory sampling strategy is presented in Goebel [1998]. A review of new proposed NRI protocols on non-federal rangelands is presented in the National Resources Inventory Handbook of Instructions for Rangeland Field Study Data Collection [USDA 2005], and a summary of NRI results on rangeland is presented in Herrick *et al*. [2010].

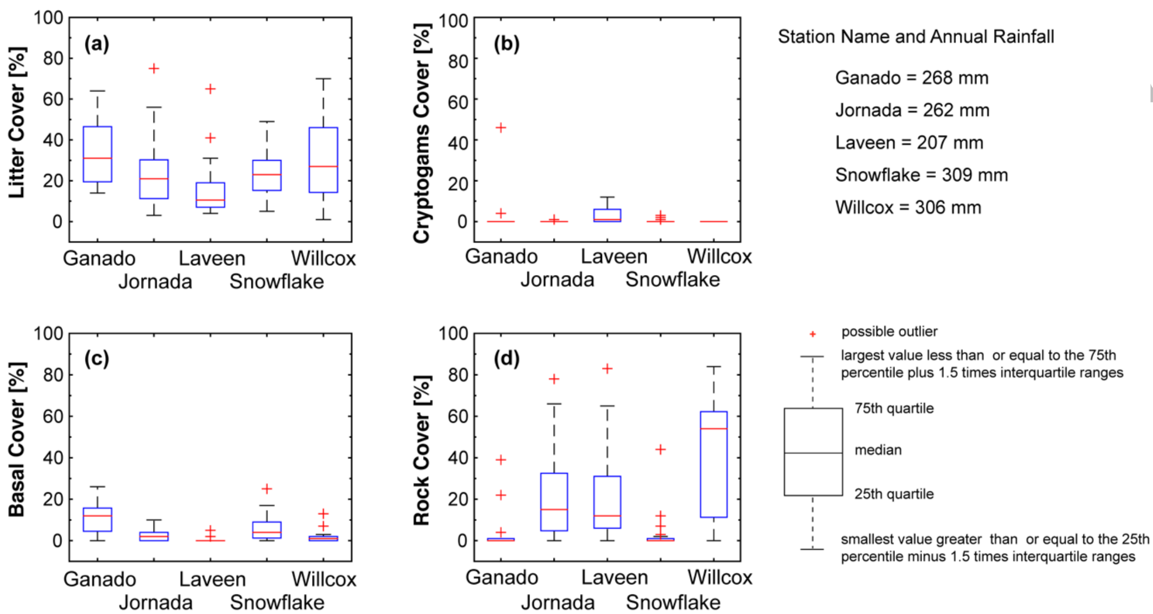

Figure 3. Distributions of ground surface cover grouped by the five weather stations. (a) Litter cover, (b) Cryptogams, (c) Basal area, and (d) Rock cover.

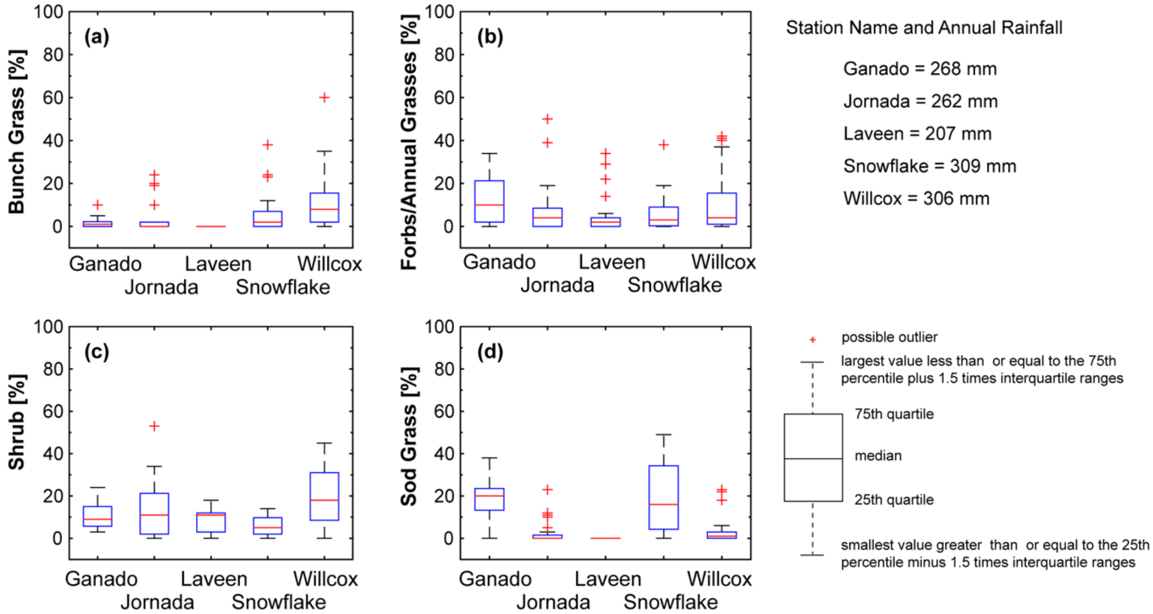

Figure 4. Distributions foliar canopy cover grouped by the five weather stations. (a) Bunch grass, (b) Forbs/Annual grasses, (c) Shrub, and (d) Sod grasses.

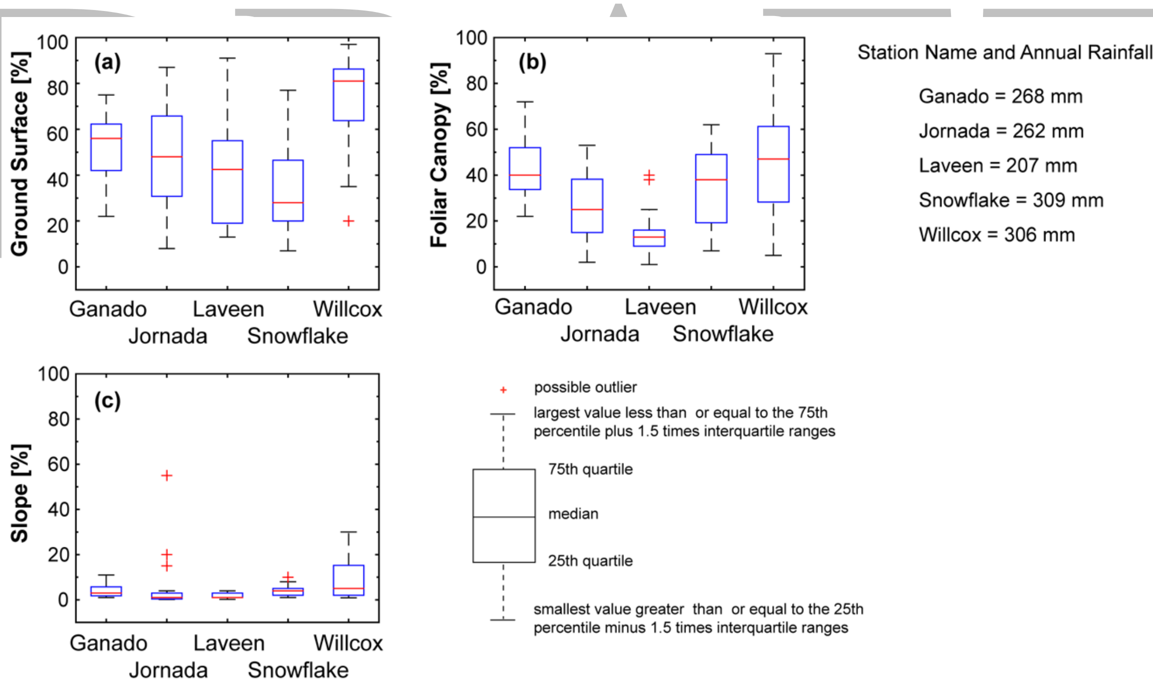

Figure 5. Distributions of total ground surface cover and foliar canopy cover grouped by the five weather stations, and slope steepness of each NRI points classified based on the weather station's radius of influence.

4. Results and Discussion

4.1. Model performance with RHEM parameter estimation equations

Total friction factor (f_t), effective saturated hydraulic conductivity (K_e), splash and sheet erodibility coefficient (K_{ss}), and concentrated flow erodibility coefficient (K_w) were estimated with the RHEM empirical equations for LH106 (Table 4). In this case we calculated K_w as the geometric mean of Equations (23) and (24).

Table 4. RHEM parameter values estimated using the empirical equations.

Parameters	Symbol	Units	Value
Total friction factor	f_t	dimensionless	5.50
Effective saturated hydraulic conductivity	K_e	(mm h^{-1})	7.29
Splash and sheet erodibility coefficient	K_{ss}	dimensionless	2661.22
Concentrated flow erodibility coefficient	K_w	(s^2 m^{-2})	8.62×10^{-6}

The model performance based on the *PBIAS* and *RSR* goodness of fit criteria for runoff volume, peak runoff, and sediment yield at LH106 is shown in Table 5.

Table 5. Model performance statistics for Lucky Hills 106.

Evaluation criteria	Runoff Volume	Peak Runoff	Sediment Yield
PBIAS (%)	2	21	-28
RSR (dimensionless)	0.49	0.57	0.58

Based on the model performance criteria reported by Moriasi *et al*. [2007], model performance based on the *RSR* criterion can be evaluated as “very good” if $0 \leq RSR \leq 0.5$ and “good” if $0.50 < RSR \leq 0.60$. Therefore, these rankings suggest that RHEM performance can be evaluated as “very good” for runoff volume, and “good” for peak runoff and sediment yield. However, based on Moriasi *et al*., (2007) *PBIAS* criterion, the RHEM performance can be evaluated for runoff volume and peak runoff as “very good’ if $PBIAS < \pm 10$, “good” if $\pm 10 \leq PBIAS \leq 15$, and “satisfactory if $\pm 15 \leq PBIAS \leq 25$, and for sediment yield can be evaluated as “good” if $\pm 15 \leq PBIAS \leq 30$. These criteria suggest that RHEM can be evaluated as ‘very good’ for runoff volume, “satisfactory” for peak runoff, and “good” for sediment yield.

Positive *PBIAS* values indicate model underestimation bias, and negative values indicate overestimation bias [Gupta *et al*., 1999]. It is apparent from Figure 6(a) that the model performance for runoff volume prediction is poor with small events and improves with large events, which is common for models [Nearing, 2000]. Figure 6(b) shows strong under prediction of peak runoff among 14 runoff events, whereas sediment yield is in general over predicted for the small events in Figure 6(c). One explanation for this behavior could be attributed to K_w; that is, it was estimated by calculating the geometric mean between the equations (23) and (24) developed by Al-Hamdan et al., [2012b]. Equation (23) estimates K_w as a function of litter, rock, clay and silt, and Equation (24) based on litter, basal, clay, and silt. Al-Hamdan et al. [2012b] proposed these equations to estimate average erodibility for a wide range of undisturbed rangeland sites. The K_w estimates computed using Equations (23) and (24) for LH106 are as follows: 4.37 x 10^{-6} (s^2 m^{-2}) and 1.70 x 10^{-5} (s^2 m^{-2}), respectively. K_w estimated by Equation (24) is nearly four times the estimated by Equation (23). Therefore, we calculated the geometric mean [8.62 x 10^{-6} (s^2 m^{-2})] and kept it constant in the analysis. The approach of estimating K_w could introduce some bias in the estimation of sediment yield.

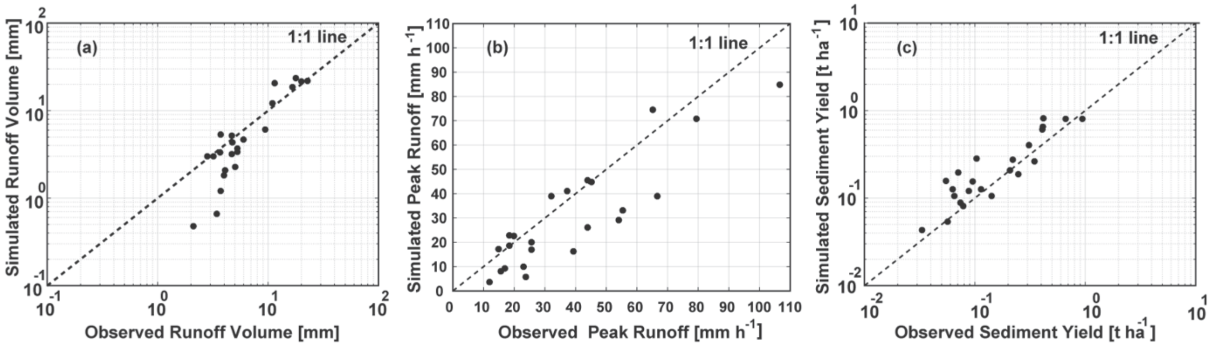

Figure 6. Comparison between observed and simulated results for each rainfall-runoff event at Lucky Hills 106: (a) Runoff volume, (b) Peak runoff and (c) Sediment yield. The parameters for these simulations were based on the RHEM parameter estimation equations.

Based on the criteria for assessing goodness of fit of the model reported in Table 5 and the 1:1 line in Figure 6, it is reasonable to conclude that RHEM is a tool that can be used for relative change analysis for comparing erosion rates of different plant functional types (bunchgrass, shrub, forb/annuals, and sod grasses).

4.2. Model calibration

The calibration process was carried out using PEST; therefore, each calibrated parameter had a different value for different rainfall events on LH106. For most events, parameters were calibrated within eight iterations, with a maximum number of 15 iterations. NSE for cumulative runoff volume ranges from 0.85 to 0.99 with a mean of 0.96, as there are ten runoff data points and four calibrated parameters per event in the hydrology component of RHEM. The RHEM calibration produced the following average values of overland flow parameters: Total friction factor f_t=3.10 (dimensionless), K_e = 6.26 (mm h^{-1}), and net capillary drive G=90 (mm). The calculated parameters by the parameter estimation equations were as follows: Total friction factor f_t = 2.60 (dimensionless) and K_e=7.29 (mm h^{-1}). The calibrated net capillary drive G value (90 mm) was smaller than the recommended in the KINEROS2 manual (127 mm) and reported by Rawls *et al*. [1982] for a sandy loam soil texture class.

The calibration of K_{ss} for each soil erosion event using PEST was achieved as follows. Total friction factor, effective saturated hydraulic conductivity, capillary drive and Kw remained fix for every calibration run. For most events K_{ss} was calibrated within three or five iterations. NSE for cumulative soil loss ranges from 0.81 to 0.96 with a mean of 0.90. The mean calibrated K_{ss} was 2089 (m^2 s^{-2}), which is lower than the value estimated by the equations proposed by Al-Hamdan *et al*. [2016] as reported in Table 4.

4.3 Model Evaluation using NRI data

This section reports the effects of ground cover on total friction factor (f_t), effective saturated hydraulic conductivity (K_e), and splash and sheet erodibility factor (K_{ss}) estimated using the parameter estimation equations.

To investigate the effect of foliar canopy cover and ground cover on sediment yield on the 124 NRI points, the RHEM model was run for a 300-year synthetic rainfall sequence generated by CLIGEN V5.3 [Nicks *et al*., 1995] based on the statistics of historic rainfall at each climate station.

The associations between ground cover and $\log_{10}(f_t)$, K_e, and K_{ss} are shown in Figure 7. They provide a basis for evaluating the behavior of the parameter estimation equations. That is, $\log_{10}(f_t)$ increased with increasing ground cover as shown in Figure 7(a), the strong positive correlation coefficient (r= 0.79, $p < 0.05$), suggesting that the parameter estimation equation to predict total friction roughness was not affected by outliers or small departures from model assumptions. For example, a slope steepness of 55% was reported in one NRI plot as shown in Figure 5(c). Similarly, we expected that K_e would increase with increased litter cover and basal area cover as shown in Figure 7(b). Although the spread of K_e around 80% ground cover, with the moderate correlation coefficient (r=0.46, $p < 0.05$), suggests that the parameter estimation equation for predicting K_e for a sandy loam soil texture class was not affected by small departures from model assumptions. The rate of rapidly increasing K_{ss} starts at about 35% ground cover; this threshold value is consistent with several studies which concluded that erosion to runoff ratio increases substantially when bare ground exceeds 50% [e.g. Al-Hamdan *et al*., 2013; Pierson *et al*. 2013]. This is supported by Gifford's [1985] and Weltz *et al*. [1998] extensive reviews of the literature on rangeland cover, which concluded that ground cover should be maintained above a critical threshold of ~50-60% to protect the soil surface adequately. A strong negative Spearman correlation coefficient (rho = -0.71, $p < 0.05$) and a fitted decaying exponential model ($R^2 = 0.82$, $p < 0.05$) to the data shown in Figure 7(c) confirms the expected decreasing monotonic trend between ground cover and K_{ss}, and the NRI point with 55% slope did not appear to cause an adverse effect on the correlation coefficient and fitted decaying exponential model.

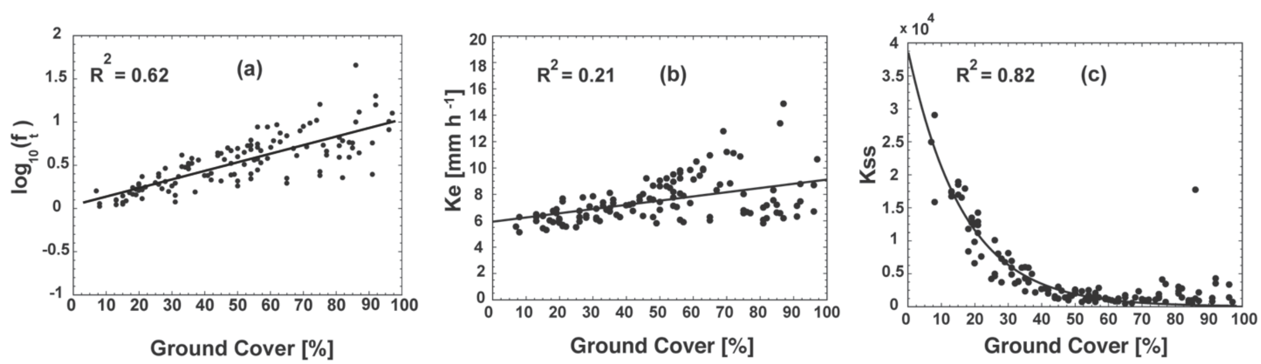

Figure 7. The association between ground cover and total friction factor (f_t), effective saturated hydraulic conductivity (K_e) and splash and sheet erodibility coefficient (K_{ss}). (a) strong positive linear correlation between ground cover and $\log_{10}(f_t)$, (b) moderate linear correlation between

ground cover and K_e, and (c) strong Spearman rank correlation coefficient between ground cover and K_{ss}.

Given that vegetation contributes much to the hydrologic and hydraulic properties of the surface, it is logical to account for the vegetation in the surface runoff process. To investigate the influence of litter and basal cover on percent runoff, defined as the ratio of runoff to precipitation, we found a strong negative linear correlation ($r = - 0.70$, $p < 0.05$) with litter as depicted in Figure 8(a). Furthermore, two distinct patterns of percent runoff emerged as a function of annual rainfall amount observed at the Ganado and Willcox weather stations. That is, both weather stations' area of influence had similar amounts of litter cover percent (Ganado: mean=34% and Willcox: mean=31%), but distinct annual rainfall regimes (Ganado: 268 mm and Willcox: 306 mm). Furthermore, the Ganado's area of influence is characterized by sod grasses (mean=19%) and forb/annual grasses (mean=12%), and the Willcox's area is characterized by a combination of shrub (mean=19 %), bunch grasses (12%), and forb/annual grasses (mean=11%). The Laveen weather station has the lowest annual rainfall amount (207mm) and the lowest litter cover percent (16%), and it is mainly shrub-forb/annual grasses-dominated (mean=9% and mean=6%, respectively).

To investigate the influence of basal cover on percent runoff, we found a moderate negative relationship depicted in Figure 8(b). Although no patterns emerged in this relation, the model was able to capture the influence of basal dynamics by showing a negative trend.

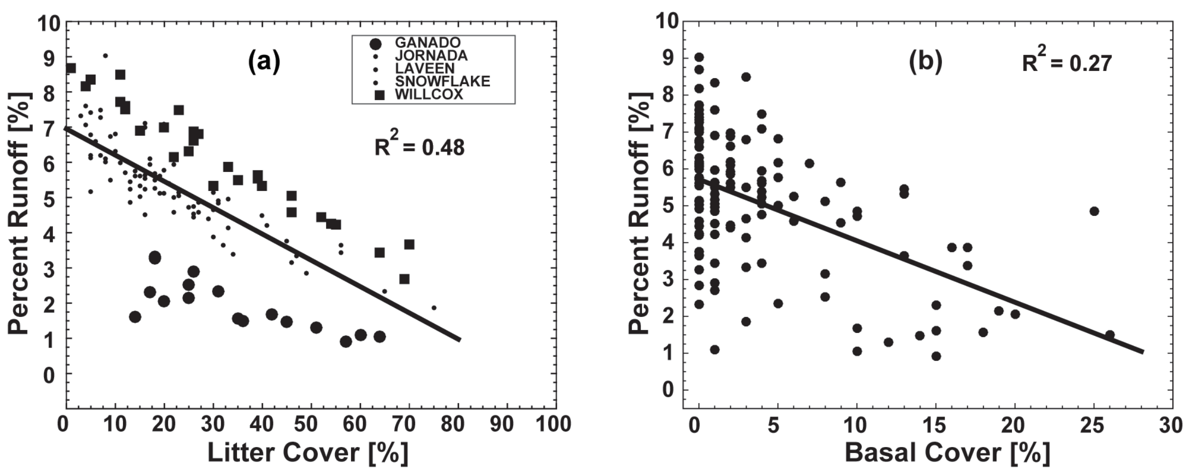

Figure 8. Runoff as a percent of precipitation showing the negative relationship with (a) litter cover percent and (b) basal cover percent.

We estimated the correlation coefficient to measure the strength of association between average annual sediment yield and the variables foliar canopy cover and ground cover, and grouped by weather stations. The results are shown in Figure 9. The strength of association between average annual sediment yield and the variable foliar canopy cover is poor, it ranged from -0.41 to -0.30 (Fig. 9(g)(i)); however, for the Ganado and Jornada weather stations the association was positive, which contradicts what would expect for this association, and for the Laveen station there is no linear relationship between the variables. One possible explanation for the behavior of this relation is the low yearly sediment yield (mean=0.16 t ha^{-1}) produced under the Ganado annual rainfall regime. In contrast, the mean yearly sediment yield for the Snowflake and Willcox weather stations were as follows 0.88 t ha^{-1} and 0.59 t ha^{-1}, respectively. These results suggest that low yearly sediment yield, in general, is not well described by foliar canopy cover. According to the boxplots shown in Fig 5c, three NRI plots were considered as possible outliers within the Jornada weather station area of influence, which may have a strong effect on the sediment yield predictions.

Likewise, we computed the correlation coefficient to investigate the strength of the association between yearly sediment yield and ground cover percent (Fig. 9). We found that the association is stronger with ground cover than with foliar canopy cover, which is expected [e.g., Nearing *et al*., 2005]. A moderate positive association was found with NRI plots within the Jornada weather station's area of influence (Fig. 9d), the steep slope argument could be made here to explain the positive trend. However, steep slopes were found in NRI plots within the Willcox weather station's area of influence (20% < slope < 30%) and the association between yearly sediment yield and foliar canopy cover was negative and ground cover was positive. The results suggest that ground cover, in general, is more highly associated with yearly sediment yield than is foliar canopy cover.

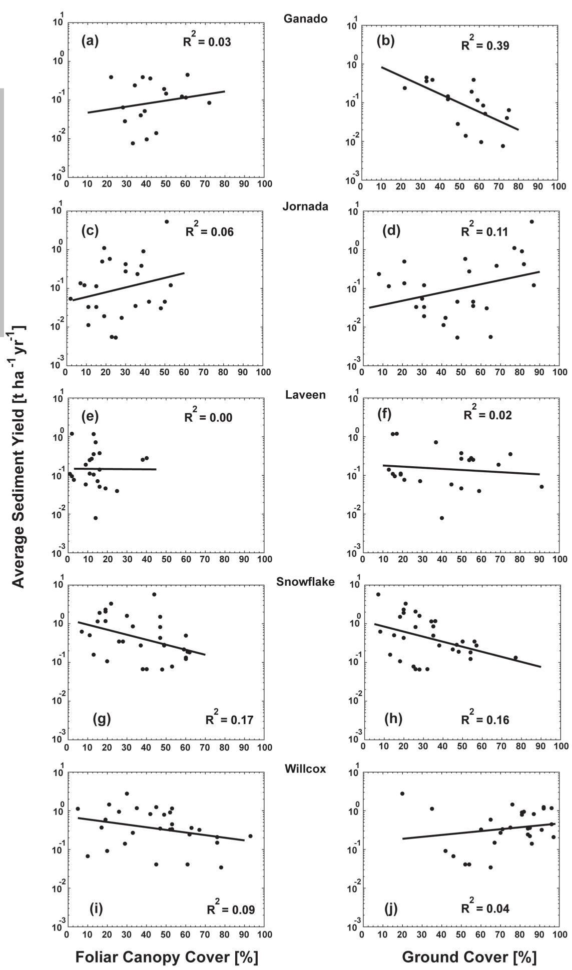

Figure 9. Association between average sediment yield and foliar canopy cover and ground cover

5. Conclusions

Reliable parameter inference is critical for meaningful prediction of soil erosion models. The capability of RHEM for simulating flow and soil erosion was tested on a small watershed in Arizona and on 124 NRI plots placed in Arizona and New Mexico. In particular, we were interested in evaluating the parameter estimation equations for predicting total friction factor (f_t), effective saturated hydraulic conductivity (K_e), splash and sheet erodibility coefficient (K_{ss}), and concentrated flow erodibility coefficient (K_w).

The performance of the model for predicting runoff volume, peak runoff, and sediment yield using the parameter estimation equations in 23 events at LH106 is as follows. Based on the RSR criterion [Moriasi *et al*., 2007], model performance is “very good” for runoff volume, and “good” for peak runoff and sediment yield. However, based on the *PBIAS* criterion [Moriasi *et al*., 2007], the performance of the model can be evaluated as ‘very good’ for runoff volume, “satisfactory” for peak runoff, and “good” for sediment yield. We achieved acceptable goodness of fit for runoff volume and sediment yield in the model calibration at LH106 on 23 events, the level of calibration was quantified with the Nash and Sutcliffe efficiency coefficient.

We compared the parameters calculated by the parameter estimation equations with the calibrated parameters at LH106. The parameter values calculated with the parameter estimation equations fell within the lowest and highest calibrated values of each parameter. The ability of the parameter estimation equations to adequately produce parameter values for the application of RHEM on a small watershed suggest that the model is well suited for small subwatersheds, provided that gully erosion is not the main active process in the watershed.

It should be noted that we kept K_w (8.62 x 10^{-6} m^2 s^{-2}) constant to avoid over-parameterization and cause adverse effects on model soil erosion predictive capacity. Runoff generation and sediment predictions are simulated in the model with separate functions, but we assumed that splash and sheet and detachment by concentrated flow are processes acting simultaneously in rangelands. Therefore, particular attention is needed as to whether Kw remains constant in further applications of RHEM outside of Lucky Hills environment.

We selected 124 NRI points in Arizona and New Mexico and ran those points through RHEM to estimate runoff and sediment yield. The NRI points were placed into five groups according to the weather station’s area of influence. The results suggest that the parameter estimation equations conveyed coherent information to the model. That is, moderate and strong negative correlation coefficients between ground cover percent and total friction factor, effective hydraulic conductivity, and splash and sheet erodibility coefficient were achieved. Likewise, moderate and strong negative correlation coefficients were found between litter cover and basal cover percent and percent runoff. In contrast, weak and moderate negative correlation coefficients were found between foliar canopy cover and ground cover and sediment yield, in the Jornada weather station group, the correlation coefficient was weak and positive. Lack of information on this location prevents further analysis as to explain the behavior of the weak positive trend between the foliar canopy and ground cover variables and sediment yield. We noticed NRI points having large slopes (55 %) in this area and considered as possible outliers, these inconsistencies in the data may be transferred and amplified in the sediment yield simulations.

Evaluation of the model predictions undertaken in this study demonstrates that RHEM produces results of satisfactory quality when simulating large flow and soil erosion events, but a greater degree of uncertainty is associated with predictions of small runoff and soil erosion events.

A high level of empirical knowledge and, in particular, prior knowledge of rangeland, management practices, soil and climatic conditions is a big advantage during all phases of the RHEM modeling, from hillslope characterization to interpretation of results.

References

Al-Hamdan O. Z, F. B. Pierson, M. A. Nearing, C. J. Williams, M. Hernandez, J. Boll, S. K. Nouwakpo, M. A. Weltz, and K. E. Spaeth (2016), Developing a parameterization approach of soil erodibility for the Rangeland Hydrology and Erosion Model (RHEM). Journal of the American Society of Agricultural and Biological Engineers, (in press).

Al-Hamdan O. Z, F. B. Pierson, M. A. Nearing, J. J. Stone, C. J. Williams, C. A. Moffet, P. R. Kormos, J. Boll, and M. A. Weltz (2012a), Characteristics of concentrated flow hydraulics for rangeland ecosystems: implications for hydrologic modeling. Earth Surface Processes Landforms 37: 157–168.

Al-Hamdan, O. Z., F. B. Pierson, M. A. Nearing, C. J. Williams, J. J. Stone, P. R. Kormos, J. Boll, and M. A. Weltz (2012b), Concentrated flow erodibility for physically based erosion models: Temporal variability in disturbed and undisturbed rangelands. Water Resources Research. 48, W07504.l

Al-Hamdan, O., F. B. Pierson, M. A. Nearing, C. J. Williams, J. J. Stone, P. R. Kormos, J. Boll, M. A. Weltz (2013), Risk assessment of erosion from concentrated flow on rangelands using overland flow distribution and shear stress partitioning. Transactions of the ASABE. 56(2):539-548.

Al-Hamdan, O.Z., M. Hernandez, F. B. Pierson, M. A. Nearing, C. J. Williams, J. J. Stone, J. Boll, and M. A. Weltz (2014), Rangeland Hydrology and Erosion Model (RHEM) enhancements for applications on disturbed rangelands. Hydrological Processes. DOI: 10.1002/hyp.10167.

Bennett, J. P. (1974), Concepts of mathematical modeling of sediment yield. Water Resources Research 10(3):485-492.

Briske, D.D., L. W. Jolley, L. F. Duriancik, and J. P. Dobrowolski (2011), Introduction to the Conservation Effects Assessment Project and Rangeland Literature Syntheses. In: Conservation Benefits of Rangeland Practices, USDA-NRCS.

Bulygina, N.S., M. A. Nearing, J. J. Stone, and M. H. Nichols (2007), DWEPP: A dynamic soil erosion model based on WEPP source terms. Earth Surface Proceses and Landforms. 32:998-1012.

Cannon, S.H., Kirkham, R.M., Parise, M., 2001a. Wildfire-related debris flow initiation processes, Storm King Mountain, Colorado. Geomorphology 39, 171 – 188.

Cerda`, A., 1998. Post-fire dynamics of erosional processes under Mediterranean climatic conditions. Zeitschrift fu¨ r Geomorphologie 42, 373 – 398.

Dortignac, E. J. and L. D. Love, (1961) Infiltration studies on ponderosa pine ranges of Colorado. Rocky Mountain Forest and Range Exp. Sta., Pap 59, 34p.

Fair, G. M., J. C. Geyer, and D. A. Okun, (1966) Water and Wastewater Engineering, Volume 1: Water Supply and Wastewater Removal, John Wiley & Sons Inc.; 1St Edition.

Flanagan, D. C., and M. A. Nearing, eds. 1995. USDA Water Erosion Prediction Project Hillslope Profile and Watershed Model Documentation. NSERL Report No. 10. West Lafayette, Ind.: USDA-ARS National Soil Erosion Research Laboratory.

Foltz, R.B., H. Rhee and W.J. Elliot. 2008. Modeling changes in rill erodiblity and critical shear stress on native surface roads. Hydrologic Processes 22:4783-4788.

Foster GR. 1982. Modeling the erosion process. In Hydrologic Modeling of Small Watersheds, ASAE Monograph 5, Haan CT (ed.). ASAE: St. Joseph, MI; 297–360

Goebel, J.J., and K.O. Schmude. 1980. Planning the SCS national resource inventory. In Arid Land Resource Inventories: Developing Cost-Efficient Methods. General Technical Report WO-28. U.S. Department of Agriculture, Forest Service, Washington, D.C. pp. 148-153.

Goebel, J. J. (1998) The National Resources Inventory and its role in U.S. agriculture, Agricultural Statistics 2000, International Statistical Institute, Voorburg, The Netherlands, 181-192.

Green W. H. and A. G. Ampt (1911), Studies of soil physics, part I – the flow of air and water through soils. Journal of Agricultural Science 4: 1–24.

IRWET and NRST, (1998), Interagency Rangeland Water Erosion Project report and state data summaries. Interagency Rangeland Water Erosion Team (IRWET) and National Rangeland Study Team (NRST). NWRC 98-1. Boise, Idaho: USDA-ARS Northwest Watershed Research Center.

Kalin L, R. S. Govindaraju, and M. M. Hantush (2004), Development and application of a methodology sediment source identification. 1: Modified unit sedimentograph approach. Journal of Hydrologic Engineering, ASCE 9(3): 184–193

Lane, L.J., M. Hernandez, and M. H. Nichols (1997), Dominant processes controlling sediment yield as functions of watershed scale. Proc. MODSIM 97, Internat'l. Conf. on Modelling and Simulation, Dec. 8-11, Hobart, Tasmania, A.D. McDonald and M. McAleer (eds.), Vol. 1, 5 pp.

Havstad, K.M., Deb Peters, B. Allen-Diaz, B. T. Bestelmeyer, D. Briske, J. L. Brown, M. Brunson, J. E. Herrick, P. Johnson, L. Joyce, R. Pieper, A. J. Svejcar, J. Yao, J. Bartolome, and L. Huntsinger (2009), The western United States rangelands, a major resource. In: Grassland, Quietness and Strength for a New American Agriculture, Chapter 5

Hernandez, M., M. A. Nearing, J. J. Stone, G. Armendariz, F. B. Pierson, O. Z. Al-Hamdan, C. J. Williams, K. E. Spaeth, M. A. Weltz, H. Wei, P. Heilman, and D. C. Goodrich (2015), Web-Based Rangeland Hydrology and Erosion Model. Proceedings

Hernandez, M., M.A. Nearing, F.B. Pierson, C. J. Williams, K. E. Spaeth, and M. A. Weltz, M.A. 2016. A risk-based vulnerability approach for rangeland management. In: Proceedings of the 10th International Rangeland Congress, The Future Management of Grazing and Wild Lands in a High Tech World, July 17-22, 2016, Saskatoon, SK, Canada. p. 1014-1015.

Hernandez, M., M. A. Nearing, J. J. Stone, F. B. Pierson Jr., H. Wei, K. E. Spaeth, P. Heilman, M. A. Weltz, and D. C. Goodrich (2013), Application of a rangeland soil erosion model using NRI data in southeastern Arizona. Journal of Soil and Water Conservation. 68(6):512-525.

Keefer, T.O., K. G. Renard, D. C. Goodrich, P. Heilman, and C. L. Unkrich (2015), Quantifying Extreme Precipitation Events and their Hydrologic Response in Southeastern Arizona. Journal of Hydrologic Engineering. 21(1): 1-10. 10.1061/(ASCE)HE.1943-5584.0001270.

Kustas, W.P. and D. C. Goodrich (1994), Preface for the Monsoon '90 multidisciplinary field campaign. Water Resour. Res. 30(5):1211-1225.
Morris, S.E. and T. A. Moses (1987), Forest fire and the natural soil erosion regime in the Colorado Front Range. Annals of the Association of American Geographers 77, 245 – 254.

Meeuwig, R. O. (1969), Infiltration and Soil Erosion as Influenced by Vegetation and Soil in Northern Utha, Journal of Range Management, 23:185-189

Morris, S.E., and T. A. Moses, (1987) Forest fire and the natural soil erosion regime in the Colorado Front Range. Annals of the Association of American Geographers 77, 245 – 254.

Nearing, M.A. 2000. Evaluating soil erosion models using measured plot data: Accounting for variability in the data. Earth Surface Processes and Landforms. 25:1035-1043.

Nearing, M.A., V. Jetten, C. Baffaut, O. Cerdan, A. Couturier, M. Hernandez, Y. Le Bissonnais, M.H. Nichols, J.P. Nunes, C.S. Renschler, V. Souchère, and K. van Oost. (2005), Modeling response of soil erosion and runoff to changes in precipitation and cover. Catena 61(2-3):131–154.

Nearing, M.A., M. H. Nichols, J.J. Stone, K.G. Renard, and J.R. Simanton (2007), Sediment yields from unit-source semi-arid watersheds at Walnut Gulch. Water Resources Research 43:W06426, doi:10.1029/2006WR005692.

Nearing, M.A. and P. B. Hairsine (2011), The Future of Soil Erosion Modelling. Ch. 20 In: Morgan, R.P. and M.A. Nearing (eds.). 2011. Handbook of Erosion Modelling. ISBN: 978-1-051-9010-7. 416 pgs. Wiley-Blackwell Publishers, Chichester, West Sussex, UK. pps. 391-397.

Nearing, M.A., H. Wei, J. J. Stone, F. B. Pierson, K. E. Spaeth, M. A. Weltz, D. C. Flanagan, and M. Hernandez (2011) A Rangeland Hydrology and Erosion Model. Trans. American Society Agricultural Engineers. 54(3): 901-908.

Nearing, M.A., F. F. Pruski, and M. R. O'Neal (2004), Expected climate change impacts on soil erosion rates: A review. J. Soil and Water Cons. 59(1):43-50.

Nearing M. A., L. D. Norton, D. A. Bulgakov, G.A. Larionov, L. T. West, and K. M. Dontsova (1997), Hydraulics and erosion in eroding rills. Water Resources Research 33: 865–876.

Nichols, M.H., M.A. Nearing, V.O. Polyakov, J.J. Stone (2012), A sediment budget for a small semiarid watershed in southeastern Arizona, USA. Geomorphology 180: 137-145 DOI: 10.1016/j.geomorph.2012.10.002.

Parlange, J.Y., I. Lisle, R. D. Braddock, and R. E. Smith, (1982), "The three-parameter infiltration equation." Soil Science, 133(6), pp337-341.

Pierson, F.B., D. H. Carlson, and K. E. Spaethe (2002), Impacts of wildfire on soil hydrological properties of steep sagebrush-steppe rangeland. International Journal of Wildfire 11, 145 – 151.

Pierson, F. B., J. D. Bates, T. J. Svejcar, and S. P. Hardegree (2007), Runoff and erosion after cutting western juniper, Rang. Ecology Manage., 60, 285–292. -- Highlighted Sep 6, 2016

Pierson, F.B., P. R. Robichaud, C. A. Moffet, K. E. Spaeth, S. P. Hardegree, P. E. Clark, and C. J. Williams (2008), Fire effects on rangeland hydrology and erosion in a steep sagebrush-dominated landscape. Hydrological Processes 22, 2916–2929.

Pierson, F. B., C. A. Moffet, C. J. Williams, S. P. Hardegree, and P. Clark (2009), Prescribed-fire effects on rill and interrill runoff and erosion in a mountainous sagebrush landscape, Earth Surf. Processes Landforms, 34,193–203.

Pierson, F. B., C. J. Williams, P. R. Kormos, S. P. Hardegree, and P. E.Clark (2010), Hydrologic vulnerability of sagebrush steppe following pinyon and juniper encroachment, Rang. Ecol. Manage., 63, 614–629, doi:10.2111/REM-D-09-00148.1. -- Highlighted Sep 6, 2016.

Pierson, F.B., Carlson, D.H., Spaethe, K.E., 2002. Impacts of wildfire on soil hydrological properties of steep sagebrush-steppe rangeland. International Journal of Wildfire 11, 145 – 151.

Rawls, W. J., D. L. Brakensiek, J. R. Simanton, and D. Kho, (1990), Development of a crust factor for a Green Ampt model. Transactions of the ASAE 33(4):1224-1228

Rawls, W. J., D. L. Brakensiek and K. E. Saxton (1982) Estimation of Soil Water Properties, Transactions of the ASAE, Paper No. 81-2510.

Rawls, W. L., D. Gimenez, and R. Grossman, (1998) Use of soil texture, bulk density, and slope of the water retention curve to predict saturated hydraulic conductivity, Transactions of the ASAE 41:983-988

Renard, K.G., M. H. Nichols, D. A. Woolhiser, and H. B. Osborn (2008) A brief background on the U.S. Department of Agriculture Agricultural Research Service Walnut Gulch Experimental Watershed. Water Resources Research. Vol. 44, W05S02

Renard, K. G. (1993). “Agricultural impacts in an arid environment: Walnut Gulch case study.” Hydrol. Sci. Tech., 9(1–4), 145–190.

Renard, K.G. 1980. Estimating erosion and sediment yield from rangelands. Proc. ASCE Sym. on Watershed Manage. '80, Boise, ID, pp. 164-175.

Scott, D.F., Van Wyk, D.B., 1990. The effects of wildfire on soil wettability and hydrological behavior of an afforested catchment. Journal of Hydrology 121, 239 – 256.

Shakesby, R.A., Coelho, C. de O.A., Ferreira, A.D., Terry, J.P., Walsh, R.P.D., 1993. Wildfire impacts on soil erosion and hydrology in wet Mediterranean forest, Portugal. International Journal of Wildland Fire 3, 95 – 110

Simanton, J.R., W. R. Osterkamp, and K. G. Renard (1993), Sediment yield in a semiarid basin: Sampling equipment impacts. Proc. Yokohama, Japan Sym., Sediment Problems: Strategies for Monitoring, Prediction and Control, R.F. Hadley and T. Mizuyama (eds.), July, IAHS Pub. No. 217, pp. 3-9.

Smith, R.E., D. C. Goodrich, D. A. Woolhiser, and C. L. Unkrich (1995). KINEROS - A kinematic runoff and erosion model. Chpt. 20 In: Computer Models of Watershed Hydrology, V.P. Singh (ed.), Water Resources Publs., pp. 697-732.

Smith, R. E., C. Corradini, and F. Melone (1993), Modeling infiltration for multi-storm runoff event. Water Resour. Res., 29 (1), 133-44.

Smith, R. E. and Parlange, J.- Y (1978). A parameter-efficient hydrologic infiltration model. Water Resour. Res., 14 (3), 533-8.

Spaeth, K. E., F. B. Pierson, M. A. Weltz, and J. B. Awang, (1996), Gradient analysis of infiltration and environmental variables as related to rangeland vegetation. Trans. ASAE 39(1): 67-77.

Stone, J.J., L. J. Lane, and E. D. Shirley (1992), Infiltration and runoff simulation on a plane. Trans. ASAE 35(1):161-170.

Tromble, J. M., K. G. Renard and A.P. Thatcher, (1973) Infiltration for Three Rangeland Soil-Vegetation Complexes, Journal of Range Management, 27(4).

Wei, H., M. A. Nearing, J. J. Stone, D. P. Guertin, K. E. Spaeth, F. B. Pierson, M. H. Nichols, C. A. Moffett (2009), A new Splash and Sheet Erosion Equation for Rangelands. Soil Science of America Journal. 73:1386-1392.

Weltz, M.A., K.E. Speath, M.H. Taylor, K. Rollins, F. B. Pierson, L. W. Jolley, M. A. Nearing, D.C. Goodrich, M. Hernandez, S. Nouywakpo, C. Rossi (2014), Cheatgrass invasion and woody species encroachment in the Great Basin: benefits of conservation. Journal of Soil and Water Conservation. 69(2):39A-44A.

Weltz, M.A., M.R. Kidwell and H. D. Fox (1998), Influence of abiotic and biotic factors in measuring and modeling soil erosion on rangelands: State of knowledge. J. Range Manage. 51(5):482-495.

Williams, C.J., F.B. Pierson, P.R. Robichaud, and J. Boll. (2014), Hydrologic and erosion responses to wildfire along the rangeland–xeric forest continuum in the western US: a review and model of hydrologic vulnerability. *International Journal of Wildland Fire* 23:155-172.

Williams, C. J., F. B. Pierson, K. E. Spaeth, J. R. Brown, O.Z. Al-Hamdan, M. A. Weltz, M. A. Nearing, J. E. Herrick, J. Boll, P. R. Robichaud, D.C. Goodrich, P. Heilman, D. P. Guertin, M. Hernandez, H. Wei, S.P. Hardegree, E.K. Strand, J.D. Bates, L.J. Metz, and M.H. Nichols (2016), Incorporating hydrologic data and ecohydrologic relationships into ecological site descriptions. Rangeland Ecology and Management. 69: 4-19. http://dx.doi.org/10.1016/j.rama.2015.10.001.

Woolhiser, D.A., R. E. Smith, and D. C. Goodrich (1990), KINEROS, a kinematic runoff and erosion model: Documentation and user manual. U. S. Depart. of Agric., Agric. Res. Service, ARS-77, 130 p.

Zhang, X. C., M. A. Nearing, and L. M. Risse (1995), Estimation of Green-Ampt Conductivity Parameters: Part I. Row Crops, Transactions of the ASAE, Vol. 38(4):1069-1077.